



**HAL**  
open science

## Performance improvement with non-alloyed ohmic contacts technology on AlGaN/GaN High Electron Mobility Transistors on 6H-SiC substrate

Marie Leseq, Yassine Fouzi, Ali Abboud, N. Defrance, Francois Vaurette, Saliha Ouendi, Etienne Okada, Marc Portail, Micka Bah, Daniel Alquier, et al.

### ► To cite this version:

Marie Leseq, Yassine Fouzi, Ali Abboud, N. Defrance, Francois Vaurette, et al.. Performance improvement with non-alloyed ohmic contacts technology on AlGaN/GaN High Electron Mobility Transistors on 6H-SiC substrate. *Microelectronic Engineering*, 2023, 276, pp.111998. 10.1016/j.mee.2023.111998 . hal-04084512

**HAL Id: hal-04084512**

**<https://hal.science/hal-04084512v1>**

Submitted on 9 May 2023

**HAL** is a multi-disciplinary open access archive for the deposit and dissemination of scientific research documents, whether they are published or not. The documents may come from teaching and research institutions in France or abroad, or from public or private research centers.

L'archive ouverte pluridisciplinaire **HAL**, est destinée au dépôt et à la diffusion de documents scientifiques de niveau recherche, publiés ou non, émanant des établissements d'enseignement et de recherche français ou étrangers, des laboratoires publics ou privés.

## Performance improvement with non-alloyed ohmic contacts technology on AlGaN/GaN High Electron Mobility Transistors on 6H-SiC substrate

Marie Lesecq<sup>1\*</sup>, Yassine Fouzi<sup>1</sup>, Ali Abboud<sup>1</sup>, Nicolas Defrance<sup>1</sup>, François Vaurette<sup>1</sup>, Saliha Ouendi<sup>1</sup>, Etienne Okada<sup>1</sup>, Marc Portail<sup>2</sup>, Micka Bah<sup>3</sup>, Daniel Alquier<sup>3</sup>, Jean-Claude De Jaeger<sup>1</sup>, Eric Frayssinet<sup>2</sup>, Yvon Cordier<sup>2</sup>

\*Corresponding author: marie.lesecq@univ-lille.fr

<sup>1</sup>Univ. Lille, CNRS, Centrale Lille, Univ. Polytechnique Hauts-de-France, UMR 8520 – IEMN-Institut d'Electronique de Microélectronique et de Nanotechnologie, F-59000, Lille, France

<sup>2</sup>Université Côte d'Azur, CNRS, CRHEA, rue B.Grégory, 06560 Valbonne, France

<sup>3</sup>GREMAN, Université de Tours, INSA Centre Val de Loire, 37071 Tours, France

### ABSTRACT

Keywords :  
HEMT  
GaN  
Regrown  
ohmic  
contacts

In this paper, non-alloyed ohmic contacts regrown by molecular beam epitaxy (MBE) are fabricated on AlGaN/GaN high-electron-mobility transistors on 6H-SiC substrate. Low ohmic contact resistance of 0.13  $\Omega$ .mm is obtained. This paper demonstrates the high frequency and high power performance improvements thanks to this technology regarding conventional technology based on alloyed ohmic contacts. The fabricated device with a 75-nm-T-shaped gate demonstrates a maximum drain current density of 1.1 A/mm at  $V_{GS} = 1$  V and a peak transconductance  $g_m$  of 464 mS/mm. A current gain cut-off frequency  $f_T$  of 110 GHz and a maximum oscillation frequency  $f_{MAX}$  of 150 GHz are achieved. At  $V_{DS} = 25$  V, continuous-wave output power density of 3.8 W/mm is achieved at 40 GHz associated with 42.8% power-added efficiency and a linear power gain of 6 dB. A maximum power-added efficiency of 55% is also obtained at  $V_{DS} = 20$  V.

### 1. Introduction

Gallium Nitride (GaN) based High Electron Mobility Transistors (HEMTs) are promising devices for developing high power RF electronics [1]. Impressive performances have been established on both Silicon (Si) [2] and Silicon Carbide (SiC) [3] substrates but highly scaled devices suffer from parasitic elements. Indeed, in order to push the limits of power-gain cut-off frequency as required for RF power applications, a key issue is to reduce the resistance  $R_C$  of source and drain ohmic contacts since it usually dominates the total parasitic resistance. Regrown ohmic contacts are commonly used to obtain lower contact resistance and to provide sharply defined ohmic edges facilitating the sub-

micron device scaling and the electrical contact with larger bandgap materials such as AlGaN [4]. Several studies have been reported with regrown N-GaN ohmic contacts by Molecular Beam Epitaxy (MBE) [5] or by Metal Organic Chemical Vapor Deposition (MOCVD) [6-7]. In this work, DC, RF pulsed and large signal measurements are reported for AlGaN/GaN HEMT on 6H-SiC substrate with N-GaN regrown ohmic contacts by MBE and with 75-nm-T-shaped-gate. The capability of this device is demonstrated for high frequency microwave power applications with a continuous wave output power density of 3.8 W/mm associated with a power added efficiency of 42.8 %.

## 2. Material growth and device technology

The HEMT structure is grown on 6H-SiC substrate by Metal Organic Chemical Vapor Deposition (MOCVD). As shown in Figure 1, the structure consists of a 2.5  $\mu\text{m}$ -thick GaN layer on a 300 nm AlN nucleation layer followed by a 12 nm-thick  $\text{Al}_{0.26}\text{Ga}_{0.74}\text{N}$  barrier capped with 3 nm-thick SiN layer.

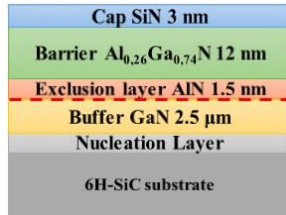


Figure 1 : Cross section view of the studied HEMT structure grown on 6H-SiC substrate

X-ray diffraction (XRD) measurements permit evaluating the crystalline quality. The peak full-width at half-maxima (FWHM) are given in table 1 and attest a good crystal quality with a threading dislocation density in GaN estimated to  $8 \cdot 10^8 \text{ cm}^{-2}$ .

XRD				
Substrate	AlN (002)	AlN (103)	GaN (002)	GaN (302)
6H-SiC	580 $^{\circ}$	648 $^{\circ}$	248 $^{\circ}$	677 $^{\circ}$

Table 1. XRD peak full width at half maximum for AlN and GaN grown on 6H-SiC substrate.

The surface morphology of the AlGaN/GaN epilayer is assessed with tapping mode Atomic Force Microscopy (AFM). A root mean square (RMS) roughness as low as 0.3 nm at small scale ( $2 \times 2 \mu\text{m}^2$  area AFM scans) is obtained (Figure 2). On  $10 \times 10 \mu\text{m}^2$  area scan, the RMS roughness is 0.7 nm.

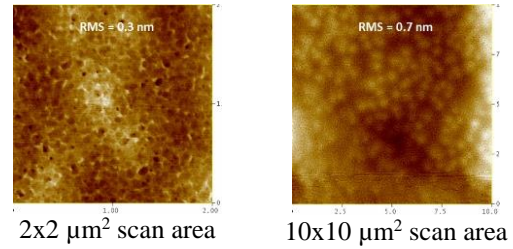


Figure 2 : AFM surface morphology of AlGaN/GaN HEMT grown on 6H-SiC substrate

An e-beam lithography based process is used to fabricate short gate length HEMTs with GaN-based regrown ohmic contacts. For comparison purposes, HEMTs are also fabricated on the same heterostructure with standard process [8] with Ti/Al/Ni/Au ohmic contacts requiring rapid thermal annealing at high temperature.

Concerning the fabrication of devices with GaN based regrown ohmic contacts, the regrowth scheme consists in selectively etching the barrier in the contact region and a few tens of nanometers of the GaN buffer, followed by the regrowth of N-doped GaN, which is then easily contacted with metal pads. The process starts with 100 nm thick HSQ (Hydrogen SilesesQuioxane) deposited by spin-coating and patterned by e-beam lithography as a mask to define source and drain contact regions to be etched. In literature, processing of HEMT with non-alloyed ohmic contacts relies on  $\text{SiO}_2$  layer obtained by PECVD and patterned by standard lithography and ICP-RIE processes, as etching mask. The HSQ based process described in this work requires only a single lithography step to define regions to be etched. With a suitable post-treatment, HSQ can have improved resistance to the etching process, almost equivalent to that of a  $\text{SiO}_2$  mask. Furthermore, its removal by wet chemical process does not present any particular difficulty and does not interfere with the GaN-based materials used.

Then, the AlGaN/GaN heterostructure is etched down to 50 nm in the source and drain contact regions by Inductively Coupled Plasma etching (ICP). A mixture of  $\text{BCl}_3/\text{Cl}_2$  gases with a ratio of 1:1 is used

as the reactive gas for GaN etching. This etching method permits to obtain vertical sidewalls and low surface damage. Highly N-doped GaN is then regrown by  $\text{NH}_3$ -source MBE around  $760^\circ\text{C}$  using a solid silicon source (SUSI) with a doping level higher to  $7 \cdot 10^{19} \text{ cm}^{-3}$  as calibrated on a separate sample. HSQ mask is removed using diluted HF solution. The following consists in the Ti/Au pad deposition on regrown ohmic contact areas. No annealing is required. The rest of the HEMT fabrication is unchanged from the standard process used at IEMN [8]. Devices isolation is performed by  $\text{N}^+$  ion multiple implantations. A Ni/Au metal stack is evaporated to form the Schottky contact. A 100 nm PECVD SiN passivation layer is deposited at  $340^\circ\text{C}$ . Finally, metallic contact pads are formed by Ti/Au evaporation. Figure 3 shows a view of the HEMT device after the microfabrication process.

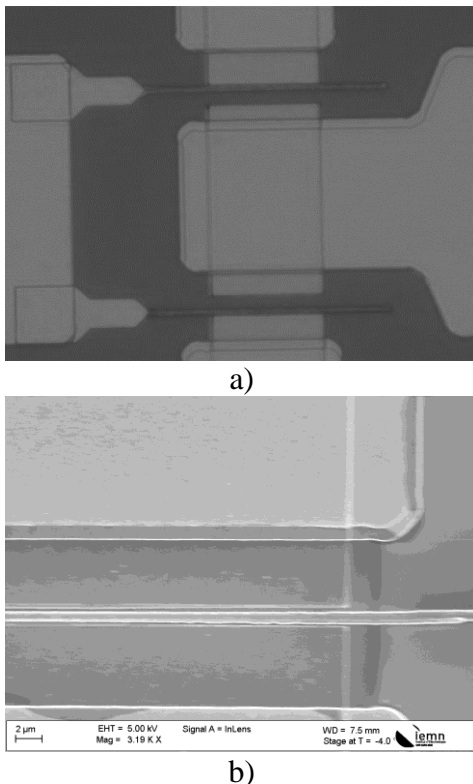


Figure 3: a) Top view of a  $2 \times 50 \times 0.075 \mu\text{m}^2$  AlGaIn/GaN HEMT on 6H-SiC substrate with non-alloyed ohmic contacts. b) SEM image of source-to-drain region and gate contact

### 3. Results and discussion

TLM measurements are used to analyze the contact resistance. A contact resistance as low as  $0.13 \Omega\cdot\text{mm}$  is reached on non-alloyed ohmic contacts. Three times reduced contact resistance is achieved as compared to standard Ti/Al/Ni/Au ohmic contacts followed by rapid thermal annealing. Hall measurements performed before passivation step reveal a sheet carrier density  $n_s$  of  $5.72 \cdot 10^{12} \text{ cm}^{-2}$  associated with a high electron mobility of  $2300 \text{ cm}^2/\text{V}\cdot\text{s}$  and a sheet resistance of  $475 \Omega$ .

Furthermore, propagation losses are measured in the 0.25-67 GHz range on coplanar waveguides fabricated on the heterostructure. The losses remain steady versus frequency and propagation losses as low as 0.25 and 0.26 dB/mm are measured at 10 GHz and 40 GHz respectively.

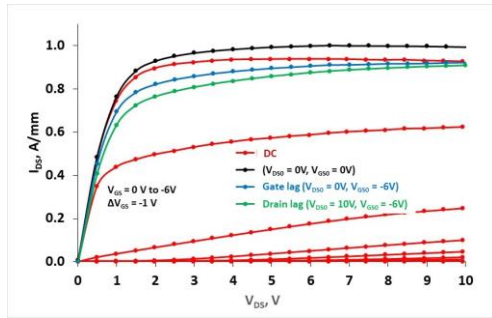
#### A. DC characteristics

Figure 4 shows pulsed and DC measurements as well as transfer characteristics for a  $2 \times 50 \times 0.075 \mu\text{m}^2$  device with non-alloyed ohmic contacts. A maximum DC current density  $I_{\text{DS,max}}$  of 0.9 A/mm is obtained at  $V_{\text{GS}} = 0\text{V}$  (1.1 A/mm is reached at  $V_{\text{GS}} = 1 \text{ V}$ ). A peak transconductance  $g_m$  of 464 mS/mm is reached at  $V_{\text{DS}} = 6\text{V}$  and  $V_{\text{GS}} = -1.4 \text{ V}$ . The  $I_{\text{ON}} / I_{\text{OFF}}$  ratio in the order of  $10^8$  is obtained.

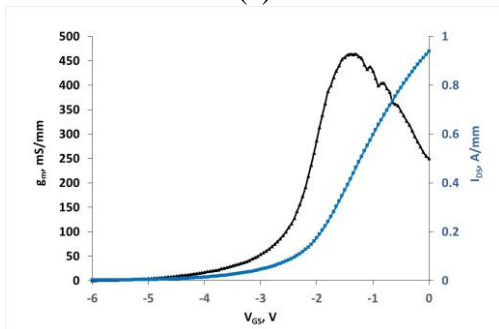
#### B. Pulsed measurement

Pulsed measurement is performed using different quiescent bias points ( $V_{\text{DS0}}$ ,  $V_{\text{GS0}}$ ) with a setup featuring 500 ns pulse duration with 0.3% duty cycle. Figure 4 shows the pulsed I-V characteristics for different quiescent bias points permitting the evaluation of the lag phenomena. At the quiescent bias point ( $V_{\text{DS0}} = 0 \text{ V}$ ,  $V_{\text{GS0}} = 0\text{V}$ ), both thermal and trapping effects are suppressed and the associated curve is used as a reference to quantify gate and drain lag effects. A current drop of 11 % is observed under gate lag condition ( $V_{\text{DS0}} = 0 \text{ V}$ ,  $V_{\text{GS0}} = -6 \text{ V}$ ). A current drop of 17 % is observed

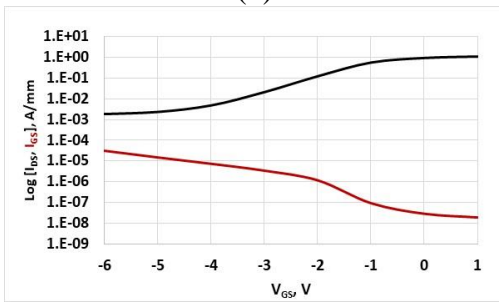
under drain lag condition ( $V_{DS0} = 10$  V,  $V_{GS0} = -6$  V).



(a)



(b)



(c)

Figure 4: Measurements on a  $2 \times 50 \times 0.075 \mu\text{m}^2$  AlGaIn/GaN HEMT on Si substrate with non-alloyed ohmic contacts : (a) DC and pulse characteristics for different quiescent bias points, (b)  $g_m(V_{GS})$  and transfer characteristics at  $V_{DS} = 6$  V, (c)  $\log[I_{DS}(V_{GS})]$  and  $\log[I_{GS}(V_{GS})]$  at  $V_{DS} = 6$  V

### C. RF characteristics

The current gain transition frequency ( $f_T$ ) and the maximum oscillation frequency ( $f_{max}$ ) are directly extracted from the first order frequency extrapolation ( $-20$  dB/decade) of current gain modulus ( $|H_{21}|$ ) and Mason's unilateral gain (U) respectively for a bias point corresponding to the peak of transconductance. At  $V_{DS} = 6$

V and  $V_{GS} = -1.4$  V, extrinsic current gain cutoff frequency  $f_T = 80$  GHz and maximum power gain cutoff frequency  $f_{max} = 150$  GHz are achieved (Figure 5).

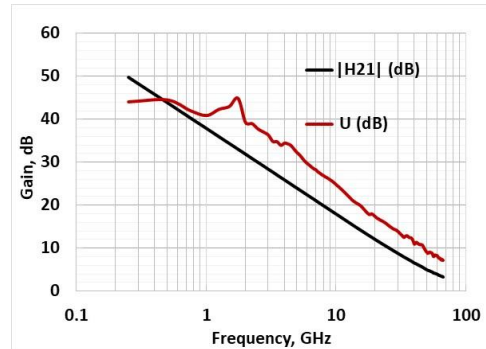


Figure 5: Current gain modulus  $|H_{21}|$ , Mason's unilateral gain (U) versus frequency for a  $2 \times 50 \times 0.075 \mu\text{m}^2$  AlGaIn/GaN HEMT on Si substrate with non-alloyed ohmic contacts at  $V_{GS} = -1.4$  V and  $V_{DS} = 6$  V.

### D. Microwave Power Measurement

Large signal characterization is performed at 40 GHz under CW condition. It is carried out with an active load-pull test bench based on a Non-linear Vectorial Network Analyzer (Keysight N5245A-NVNA). This test bench permits on-wafer large signal characterization of transistors under CW or pulsed conditions up to Q-band [9].

Figure 6 shows the CW power performance of a  $2 \times 50 \times 0.075 \mu\text{m}^2$  device with non-alloyed ohmic contacts measured for  $V_{DS}$  sweep from 10 V to 30 V.

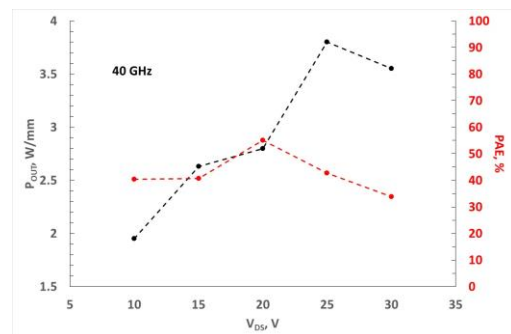


Figure 6: CW performance (Output power density and power added efficiency) as a function of a drain bias at 40 GHz measured on  $2 \times 50 \times 0.075 \mu\text{m}^2$  AlGaIn/GaN HEMT on Si substrate with non-alloyed ohmic contacts.



Figure 7 shows detailed characteristics measured at 25 V (a) corresponding to the best output power density and at 20 V (b) corresponding to the best power added efficiency. At  $V_{DS} = 25$  V and  $I_{DS} = 0.1$  A/mm, the device shows good microwave performance. The optimal impedance is  $\Gamma_L = 0.8 \angle 45^\circ$ . In these conditions, it exhibits a linear power gain  $G_p$  of 6 dB and an output power density  $P_{out}$  of 3.8 W/mm associated with a power added efficiency (PAE) of 42.8 %. Measurements are also carried out at  $V_{DS} = 20$  V and  $I_{DS} = 0.1$  A/mm with the same optimal load impedance. In this case, a linear power gain  $G_p$  of 5.3 dB and an output power density of 2.8 W/mm are obtained with a maximum PAE of 55 %.

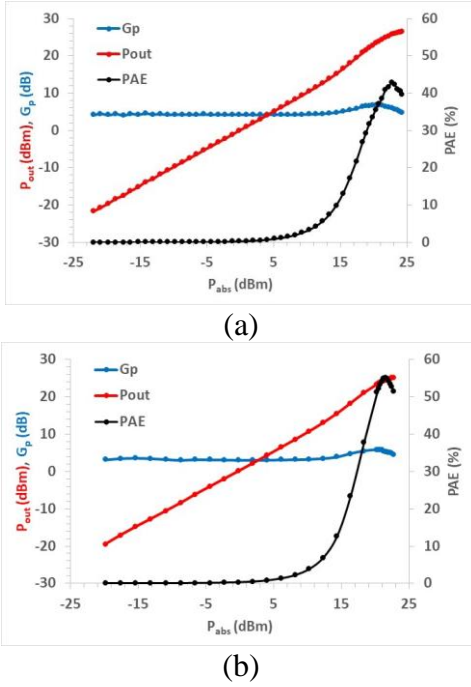


Figure 7: Output power, power gain and power added efficiency versus absorbed power at 40 GHz  $2 \times 50 \times 0.075 \mu\text{m}^2$  AlGaIn/GaN HEMT on Si substrate with non-alloyed ohmic contacts at  $V_{DS} = 25$  V (a) and at  $V_{DS} = 20$  V (b)

### E. Performance improvement compared to alloyed ohmic contacts based technology on the same epilayer

DC, RF and pulsed results on both Ti/Al/Ni/Au alloyed and N-doped GaN regrown ohmic contacts based  $2 \times 50 \times 0.075 \mu\text{m}^2$  HEMTs are given in table 2.

	With alloyed ohmic contacts	With non-alloyed ohmic contacts
$R_C$	0.6 $\Omega$ .mm	0.13 $\Omega$ .mm
$I_{DS, \max}$	0.96 A/mm	1.1 A/mm
$g_{m, \max}$	280 mS/mm	464 mS/mm
$f_T$	70 GHz	80 GHz
$f_{MAX}$	110 GHz	150 GHz
Gate lag	45 %	11 %
Drain lag	70 %	17 %

Table 2 : performance comparison of Ti/Al/Ni/Au alloyed and N-doped GaN regrown ohmic contacts based HEMTs

Contact resistance  $R_C$  extracted from TLM measurements on alloyed and non-alloyed ohmic contacts are 0.6 and 0.13  $\Omega$ .mm respectively. Non-alloyed ohmic contacts based technology not only permits decreasing the contact resistance but also having a smooth metallic contact surface as shown in figure 3. Indeed, N-GaN regrown ohmic contacts do not require high temperature annealing leading to roughness as on alloyed ohmic contacts. A maximum drain current density ( $I_{DS, \max}$ ) of 0.96 and 1.1 A/mm is obtained for the sample with non-alloyed and alloyed ohmic contacts respectively, at  $V_{GS} = 1$  V. It clearly shows that lower contact resistance for non-alloyed ohmic contacts has significant effects on  $I_{DS}$ . The maximum transconductance  $g_m$ , obtained for the sample with non-alloyed and alloyed ohmic contacts is 280 and 464 mS/mm respectively. A higher value of  $g_m$  is important to improve RF performance. Indeed,  $f_T/f_{MAX}$  increases from 70 / 80 GHz for alloyed ohmic contacts based HEMTs to 110 GHz to 150 GHz for non-alloyed ohmic contacts based HEMTs. Observed lag effects on device with non-alloyed ohmic contacts are significantly lower than those measured on device with alloyed ohmic contacts. This observation could be attributed to the SiN cap layer removal

during the process along with the release of the HSQ layer.

#### 4. Conclusion

The N-GaN regrown non-alloyed ohmic contacts exhibited improved DC and RF performances compared with the Ti/Al/Ni/Au-based alloyed ohmic contacts. The 0.075  $\mu\text{m}$  gate length HEMTs fabricated with non-alloyed ohmic contacts exhibited a maximum power density of 3.8 W/mm at 40 GHz while the device was biased at  $V_{\text{DS}} = 25$  V with a quiescent current of 0.1 A/mm. High-power and high-frequency performance could be further improved by reducing source to gate distance which is possible thanks to the smooth surface of non-alloyed ohmic contacts. Furthermore, the non-alloyed ohmic contact based technology does not require annealing at high temperature leading the possibility to form source and drain contacts after the gate fabrication. This makes it possible the self-aligned gate process.

#### References

- [1] F. Roccaforte and M. Leszczynski, Nitride Semiconductor Technology: Power Electronics and Optoelectronic Devices, Wiley-VCH, 2020, ISBN 978-3-527-34710-0 e-ISBN 978-3-527-82525-7. hal-03287288
- [2] D. Marti et al, IEEE Electron Device Letters, Vol. 36, No. 1, January 2015, <https://doi.org/10.1109/LED.2014.2367093>
- [3] K. Shinohara et al, IEEE Transactions On Electron Devices, Vol. 60, No. 10, October 2013, <https://doi.org/10.1109/TED.2013.2268160>
- [4] I. Abid et al, Electronics 2021, 10, 635. <https://doi.org/10.3390/electronics10060635>
- [5] Y. Zhou et al, Appl. Phys. Lett., 120, 062104, 2022, <https://doi.org/10.1063/5.0079359>
- [6] L. Zhang et al, Appl. Phys. Lett., 119, 262104, 2021, <https://doi.org/10.1063/5.0077937>

[7] H. Cakmak et al, IEEE Transactions on Electron Devices, vol.68, n°3, march 202, <https://doi.org/10.1109/TED.2021.3050740>

[8] M-R. Irekti et al, 2019 Semicond. Sci. Technol. 34 12LT01,

<https://doi.org/10.1088/1361-6641/ab4e74>

[9] R. Kabouche et al, IEEE Microwave and wireless components letters, vol.27, 2017, <https://doi.org/10.1109/LMWC.2017.2678424>

#### Acknowledgments

This work was supported by the technology facility network RENATECH, the French National Research Agency (ANR) through the projects ASTRID GoSiMP (ANR-16-ASTR-0006) and the “Investissement d’Avenir” program GaNeX (ANR-11-LABX-0014). This research work was partially undertaken with the support of IEMN fabrication (CMNF) and characterization (PCMP) platforms.